Numerical assessment of the potential for future limnic eruptions at lakes Nyos and Monoun, Cameroon, based on regular monitoring data

TOMOFUMI KOZONO[1]*, MINORU KUSAKABE[2], YUTAKA YOSHIDA[3], ROMARIC NTCHANTCHO[4], TAKESHI OHBA[5], GREGORY TANYILEKE[4] & JOSEPH V. HELL[4]

[1]*Department of Geophysics, Graduate School of Science, Tohoku University, 6-3, Aramaki Aza-Aoba, Aoba-ku, Sendai, Miyagi 980-8578, Japan*

[2]*Department of Environmental Biology and Chemistry, The University of Toyama, Gofuku 3190, Toyama 930-8555, Japan*

[3]*Yoshida Consulting Engineer Office, Tsukigaoka, Morioka 020-0121, Japan*

[4]*Institute of Research for Geology and Mining, P.O.B. 4110, Yaoundé, Cameroon*

[5]*Department of Chemistry, School of Science, Tokai University, Hiratsuka 259-1211, Japan*

**Correspondence: kozono@zisin.gp.tohoku.ac.jp*

Abstract: We assessed the potential for limnic eruptions at lakes Nyos and Monoun, Cameroon on the basis of numerical modelling and CO_2 profiles obtained by regular monitoring of the lakes. The change through time of the profiles suggests one particular scenario for producing an eruption: a supply of CO_2-undersaturated fluid from the lake bottom that induces upwards growth of the CO_2-rich bottom layer, leading eventually to CO_2 saturation at mid-depths of the lake. By using a numerical model for the ascent of a plume of CO_2 bubbles, we found that under realistic conditions (e.g. a profile of CO_2 as deduced from the regular monitoring data), a bubble plume generated from the middle depths of the lake can reach the lake surface with a high flux of CO_2, which corresponds to a limnic eruption. In addition, we developed a numerical model to investigate how changes in the CO_2 concentration at the lake bottom affect the dynamics of a two-phase flow in the controlled degassing pipe, using the recently observed CO_2 profiles. This model enables us to estimate the CO_2 concentrations at the lake bottom from the heights of fountains that are observable at the lake surface.

A limnic eruption is a gas outburst from a lake (Halbwachs *et al.* 2004), and it may sometimes cause a catastrophic disaster in the surrounding area. Lakes Nyos and Monoun in Cameroon, Central Africa, are volcanic crater lakes where limnic eruptions with catastrophic releases of CO_2 gas occurred in 1986 (Lake Nyos) and 1984 (Lake Monoun), causing disasters that together claimed close to 1800 lives (Sigurdsson *et al.* 1987; Sigvaldason 1989). To understand the mechanism of the limnic eruptions in these lakes, chemical measurements of the lake water were conducted (e.g. Kling *et al.* 1989; Kusakabe *et al.* 1989, 2000, 2008; Giggenbach 1990; Evans *et al.* 1994), and numerical modelling of the eruptions has also contributed to our understanding of their dynamics (e.g. Kantha & Freeth 1996; Zhang 1996; Woods & Phillips 1999; Schmid *et al.* 2006; Mott & Woods 2010).

The chemical measurements at lakes Nyos and Monoun revealed that a large amount of CO_2 is still stored in these lakes after the gas outbursts, and that the CO_2 profile of the lake water is characterized by a stratified structure with three main layers separated by chemoclines. The CO_2 concentration increases with depth, and some layers with a roughly constant CO_2 concentration are observed (e.g. Kusakabe *et al.* 2008). Limnic eruptions such as those of the 1980s, when there was a catastrophic release of CO_2 gas, might have been triggered when the CO_2 concentration at some depth of the lake reached saturation; consequently, precise measurements of the CO_2 profile are imperative if we are to understand the mechanisms of a limnic eruption and assess the potential for future eruptions.

Another important factor that affects the current CO_2 profiles in lakes Nyos and Monoun is the artificial removal of dissolved CO_2 ('controlled

From: OHBA, T., CAPACCIONI, B. & CAUDRON, C. (eds) 2017. *Geochemistry and Geophysics of Active Volcanic Lakes*. Geological Society, London, Special Publications, **437**, 163–175.
First published online January 19, 2016, https://doi.org/10.1144/SP437.8

degassing') using degassing pipes (Halbwachs *et al.* 2004). As CO_2-rich water is withdrawn from the deep layer through a pipe, the flow of the fluid in the pipe becomes self-sustaining because of exsolution of gas bubbles and their expansion caused by decompression in the rising water column. This leads to the formation of a fountain on the lake surface. Owing to this controlled degassing, which started in 2001 and 2003 at lakes Nyos and Monoun, respectively, the amount of CO_2 dissolved in the lake water has been dramatically reduced (Kusakabe *et al.* 2008; Kusakabe 2015). Because the dynamics of pipe flow are controlled by the deep-water CO_2 concentration, which is a boundary condition at the pipe inlet, a change in the CO_2 concentration may affect the efficiency of degassing through the pipe.

To investigate the evolution of the CO_2 profiles in lakes Nyos and Monoun, regular monitoring of the chemical composition of the lake water has been conducted since the limnic eruptions, and almost every year since 1999 (Kusakabe *et al.* 2008). This monitoring is ongoing, and the most recent data collection was made in April 2014 at both lakes. The monitoring allows us to obtain detailed information about the CO_2 profiles in the lakes with high vertical resolution (the CO_2 concentration is measured at depth intervals of 1 m), and the information is useful for investigating the mechanisms of limnic eruptions.

The numerical modelling of limnic eruptions has investigated various scenarios for the causes of the eruptions, such as the upward motion of fluid along an isolated conduit of constant radius from deep in the lake (Zhang 1996), the motion of turbulent bubble plumes accompanied by the entrainment of ambient water that contains CO_2 (Woods & Phillips 1999), roll-over or convective overturn caused by a heat flux through the lake system (Rice 2000), and the ascent of a bubble-laden discrete cloud of fluid from the base of the lake (Mott & Woods 2010). Although the modelling studies indicate that each of these scenarios could produce limnic eruptions under realistic conditions, the precise trigger for the eruptions is still under discussion.

In this article, we aim to assess the potential for limnic eruptions at lakes Nyos and Monoun through numerical modelling based on the data from the regular monitoring of the CO_2 profiles in the lakes. We show first that the evolution of the CO_2 profiles over the past 28 years, obtained by regular monitoring, indicates that there is one possible scenario for a limnic eruption: the gradual upwards growth of a CO_2-undersaturated layer starting from the bottom of the lake with subsequent bubble formation at mid-depths (Kusakabe *et al.* 2008; Kusakabe 2015). We investigate numerically whether bubble formation in this scenario leads to a bubble plume reaching the lake surface (i.e. a limnic eruption), referring to the bubble plume model of Woods & Phillips (1999). In addition, the most recent CO_2 profiles indicate a drastic decrease in the CO_2 concentration at the bottom of the lake, and we investigate how changes in the CO_2 concentrations at the bottom affect the dynamics of pipe flow, using a numerical model. Although pipe flow modelling has already been discussed briefly in previous studies (e.g. Schmid *et al.* 2006), we systematically analyse the detailed features of pipe flow and investigate how the exit velocity that influences fountain height depends on the source parameters in our original model.

Evolution of CO_2 profiles at lakes Nyos and Monoun

The monitoring data record the evolution of the CO_2 profiles at lakes Nyos and Monoun for the period 1986 to 2014 (Fig. 1). As part of regular monitoring, CO_2 concentrations were determined using three methods: the syringe method, the pH method (Kusakabe *et al.* 1989, 2000, 2008), and the gas self-lifting method (Yoshida *et al.* 2010). In the syringe method, the total dissolved carbonate ($=H_2CO_3 + HCO_3^- + CO_3^{2-}$) fixed *in situ* in a plastic syringe containing a concentrated solution of KOH was later determined in the laboratory using micro-diffusion analysis. In the pH method, the CO_2 concentration was calculated using HCO_3^- concentration, pH and the temperature measured with a CTD (conductivity–temperature–depth) profiler under the assumption that chemical equilibria had been attained among the dissolved carbonate species. In this method, because the HCO_3^- values were obtained only for depths where chemical analysis was done after water sampling, a regressed relationship between HCO_3^- concentration and electrical conductivity normalized to 25°C was used to obtain HCO_3^- concentration at any depth. In the gas self-lifting method, the volumes of gas and water phases spouting from a hose that was deployed into deep water were measured separately, and the CO_2 concentration was calculated from these volumes under the assumption that CO_2 in the water phase is in equilibrium with CO_2 gas at the measured temperature and pressure. The gas self-lifting method enabled us to obtain the CO_2 concentration at closely spaced depth intervals (every 1 m). The details of these sampling and analytical methods are described in Kusakabe *et al.* (2008) and Yoshida *et al.* (2010).

The CO_2 profiles in both lakes are characterized by a stratified structure with three main layers separated by chemoclines (Fig. 1). The concentration of CO_2 increases roughly linearly with pressure, which

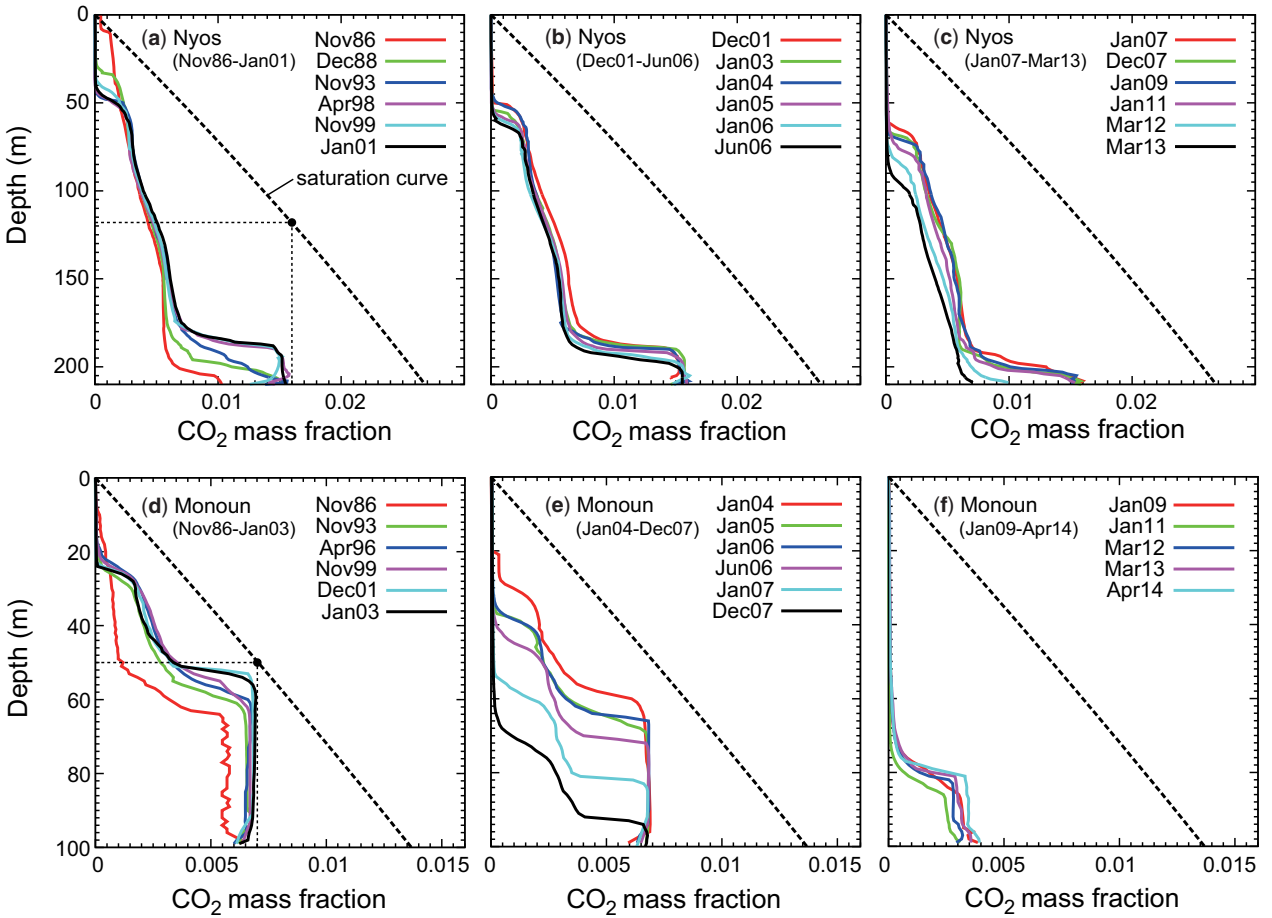

Fig. 1. Evolution of the CO_2 profiles at lakes Nyos (**a**–**c**) and Monoun (**d**–**f**) from regular monitoring data. The solubility of CO_2 in water is based on Duan & Sun (2003) and is shown as a dashed curve (saturation curve). In (**a**) and (**d**), the expected points where the CO_2 profiles reach the saturation curves because of the upwards growth of the bottom layer are represented by solid circles.

leads to a stable stratification because the density of water increases with increasing amounts of CO_2 dissolved in the water. The solubility of CO_2 in water shows a roughly linear relationship with pressure or depth (Duan & Sun 2003), as indicated by the saturation curve in Figure 1. The CO_2 profiles are below the saturation curve, indicating that the lake water is CO_2-undersaturated. As reported by Kusakabe *et al.* (2008), the CO_2 profiles have been greatly affected by controlled degassing. After the controlled degassing was started at lakes Nyos and Monoun in 2001 and 2003, respectively, the profiles and chemoclines in both lakes subsided steadily, and the total amount of dissolved CO_2 was reduced (Fig. 1b, c, e, f).

One of the notable features of the evolution of the CO_2 profiles is that the mass fraction of CO_2 in the water (i.e. CO_2 concentration) in the bottom layer does not exceed a given value (0.016 for Lake Nyos and 0.007 for Lake Monoun), which is below saturation at each lake bottom. Furthermore, before the controlled degassing, the thickness of the bottom layer increased while a constant CO_2 concentration was maintained. In Lake Monoun especially the upward growth of the CO_2 profile in the bottom layer led to near saturation at middle depths of the lake (*c.* 52 m) in 2001 and 2003 (Fig. 1d). These situations imply the following possible scenario for a limnic eruption: a continuous supply of CO_2-undersaturated fluid from the lake bottom induces the expansion of the bottom layer, leading to a CO_2 profile that reaches the saturation curve, thereby resulting in bubble formation.

An important feature of the most recent CO_2 profiles since the degassing operation is that the CO_2 mass fraction at the lake bottom has drastically decreased from 0.016 to 0.006 for Lake Nyos (Fig. 1c) and from 0.007 to 0.003 for Lake Monoun (Fig. 1f). Because the intake depths of the degassing pipes were set near the bottom (203 m water depth for Lake Nyos and 93 m for Lake Monoun, where the water depths of lakes Nyos and Monoun are about 210 and 100 m, respectively), this change in the CO_2 concentration at the bottom may affect the dynamics of pipe flow and the controlled degassing.

Plume rise induced by growth of the CO_2-undersaturated bottom layer

The potential for limnic eruptions caused by the upward growth of the CO_2-undersaturated bottom layer was deduced from the evolution of the CO_2 profiles shown in Figure 1, and this potential can also be assessed on the basis of numerical modelling. If the bottom layer grows upwards while maintaining its CO_2 mass fraction (0.016 at Lake Nyos and 0.007 at Lake Monoun), as indicated by the evolution of the CO_2 profiles before controlled degassing (see Fig. 1a, d), the CO_2 profile may reach the saturation curve at depths of about 118 m for Lake Nyos and 50 m for Lake Monoun (solid circles in Fig. 1a, d). In this article we use a numerical model to investigate how limnic eruptions can occur from these depths.

We use the one-dimensional bubble plume model developed by Woods & Phillips (1999) to investigate the dynamics of the eruptions. This model provides a numerical solution for the motion of a turbulent bubble plume from the lake bottom accompanied by the entrainment of ambient water that contains CO_2, and the model reproduces a plume erupting at the surface (a limnic eruption) if the surface flux of CO_2 is sufficiently greater than that at the bottom because of the rapid entrainment of CO_2-bearing ambient water. Since the bubble plume in the model of Woods & Phillips (1999) is generated by a continuous supply of CO_2-saturated water from a source (bottom water), we consider that their model can be used to investigate our scenario, in which a bubble plume starts rising from a mid-depth where CO_2 saturation is reached by growing CO_2-rich deep water. In the bubble plume model, the flux and velocity of the plume at the source and the CO_2 profile in the lake are given as initial conditions of calculations, and these conditions control whether a limnic eruption occurs. For example, when the CO_2 flux at the source is low, the plume loses buoyancy during the ascent, and it cannot reach the lake surface. On the other hand, when the CO_2 flux exceeds a critical value, the plume can reach the surface, leading to a limnic eruption.

As a reference calculation, we first investigated a process whereby the plume rises from the lake bottom, although we acknowledge that this process does not reflect the actual evolution of the CO_2 profiles, because the lake bottom is CO_2-undersaturated, as shown in Figure 1. In this reference calculation, the CO_2 profiles in the lake were set on the basis of the regular monitoring data (Fig. 1). We used the January 2001 profile for Lake Nyos and the January 2003 profile for Lake Monoun, just before controlled degassing, when the profiles are closest to the saturation curve (Fig. 1a, d). We also used the recent March 2013 profile for Lake Nyos and the April 2014 profile for Lake Monoun (Fig. 1c, f). Because the lake bottom has to be CO_2-saturated in order to produce the plume, we assumed a saturated layer at the lake bottom with a thickness of 1 m. On the basis of the plume model, we obtained a critical CO_2 flux at the lake bottom for the plume to reach the surface and cause a limnic eruption (Table 1). When the CO_2 flux at the lake bottom is greater than this

Table 1. *Critical CO_2 flux at the lake bottom for the bubble plume to reach the lake surface obtained from the plume model*

	Lake Nyos		Lake Monoun	
CO_2 profile	January 2001	March 2013	January 2003	April 2014
Critical CO_2 flux (kg s^{-1})	9953	21 133	303	1183
Initial plume radius (m)	10.8	15.8	2.7	5.3

The initial plume radius at the bottom for each critical flux is also shown. The initial plume velocity at the bottom and the temperature are set as 1 m s^{-1} and 298 K, respectively. Results are obtained with varying CO_2 profile in the lake based on regular monitoring data (Fig. 1).

critical value, the plume can reach the lake surface. In the case that the CO_2 profile in the lake is close to the saturation curve (January 2001 for Lake Nyos and January 2003 for Lake Monoun), the plume can entrain CO_2-rich water during ascent, which promotes further bubbling and enhances buoyancy. As a result, a critical CO_2 flux for a limnic eruption to occur becomes lower than that for the sufficiently CO_2-undersaturated recent profiles (March 2013 for Lake Nyos and April 2014 for Lake Monoun). Nevertheless, the critical CO_2 flux is higher than about 10^4 kg s^{-1} for Lake Nyos and 300 kg s^{-1} for Lake Monoun when the initial plume velocity at the lake bottom is 1 m s^{-1}, and it is much higher than the supply rates of the CO_2 into the lakes, which have been estimated to be 0.17 kg s^{-1} (120 Mmol a^{-1}) for Lake Nyos and 0.012 kg s^{-1} (8.4 Mmol a^{-1}) for Lake Monoun, based on the evolution of the total amount of CO_2 in the lakes (Kusakabe *et al.* 2008). This suggests that, under the present CO_2-undersaturated lake conditions, and without a rapid supply of CO_2, it is difficult to induce a limnic eruption by a plume rising from the lake bottom.

In our scenario, when the CO_2 profile reaches the saturation curve at the mid-depth of the lake because of the upward growth of the CO_2-undersaturated layer, the generation of a bubble plume can be deduced from the saturation point at mid-depths. However, the mechanism by which the plume is generated, and the factors that control the initial flux and velocity of the plume at the source, are unclear. Because the top of the growing CO_2-undersaturated layer corresponds to the chemocline (Fig. 1a, d), a destabilization near the chemocline is necessary. Although we have not been able to model the process that generated the plume, we will investigate in this article whether a generated plume can reach the lake surface (i.e. whether a limnic eruption occurs), and this depends on the initial flux and velocity of the plume at the source and the CO_2 profile in the lake. The mechanism of generating the bubble plume will be discussed later.

A plume rising from the middle depths of the lake can be modelled by choosing the source conditions, and we set the depth and the CO_2 mass fraction at the source as 118 m and 0.016 for Lake Nyos (Figs 1a & 2a) and 50 m and 0.007 for Lake Monoun (Figs 1d & 2b). We systematically investigated a critical CO_2 flux at the source (the mid-depth of the lake) for the plume to reach the lake surface by varying the initial velocity at the source. In our calculations, we defined that when the plume velocity falls below 0.01 m s^{-1} during ascent, the rise of the plume is stopped because any remaining bubbles may be able to separate from the fluid in the plume (Woods & Phillips 1999). The CO_2 profile in the lake between the middle depth and the surface was set by reference to regular monitoring data. We assumed a zero concentration of CO_2 in the upper layer (down to 40 − 50 m for Lake Nyos, and 15 − 25 m for Lake Monoun) and a linear increase in concentration with depth in the lower layer (down to 118 m for Lake Nyos, and 50 m for Lake Monoun), as was also assumed by Woods & Phillips (1999) (Fig. 2). The degree of saturation in the profile is parameterized by the depth at the boundary between the two layers (d_c). This depth was set close to the lowest depth of the upper chemocline in the observed CO_2 profiles (Figs 1 & 2).

Figure 3 shows the critical CO_2 flux of the plume at the source (the mid-depth of the lake), if the plume is to reach the surface by keeping the ascent velocity higher than 0.01 m s^{-1} throughout the lake, as a function of the initial velocity of the plume at the source with varying d_c. When the CO_2 flux at the source for a given initial velocity is extremely low, the initial radius of the plume becomes smaller than several millimetres, which is outside the validity of the plume model. In order to remove this unrealistic condition, in Figure 3 we also showed the relationship between the CO_2 flux at the source and the initial velocity where the initial plume radius is 1 cm (dotted line): in the range above this line the initial radius is larger than 1 cm.

The critical CO_2 flux increases with decreasing initial velocity at the source or with increasing d_c, and the effect of d_c is predominant (Fig. 3). When d_c is set close to the depth of the upper chemocline ($d_c = 45$ m for Lake Nyos and 22.5 m for Lake Monoun; Fig. 2), the critical flux is lower than the observed supply rate of CO_2 (0.17 kg s^{-1} for Lake

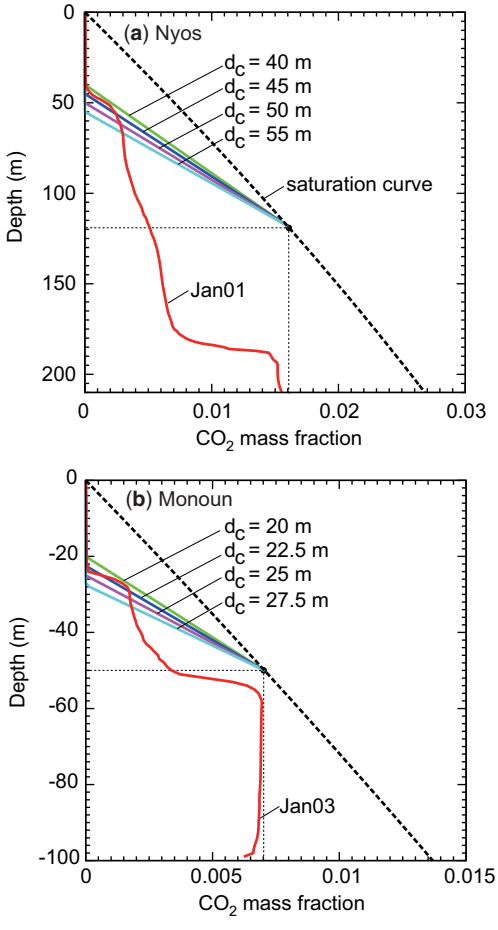

Fig. 2. CO_2 profiles assumed for calculations of plume rise from the mid-depth of lakes (**a**) Nyos and (**b**) Monoun caused by the upwards growth of the bottom layer. The profiles start from the point (solid circle) where the depths and the CO_2 mass fractions are 118 m and 0.016 in Lake Nyos, and 50 m and 0.007 in Lake Monoun. The variations in the profiles are parameterized by a depth (d_c) at the boundaries between the upper layer with zero concentration and the lower layer where the concentration increases linearly with depth. The CO_2 profiles in January 2001 at (**a**) Lake Nyos and in January 2003 at (**b**) Lake Monoun are also shown.

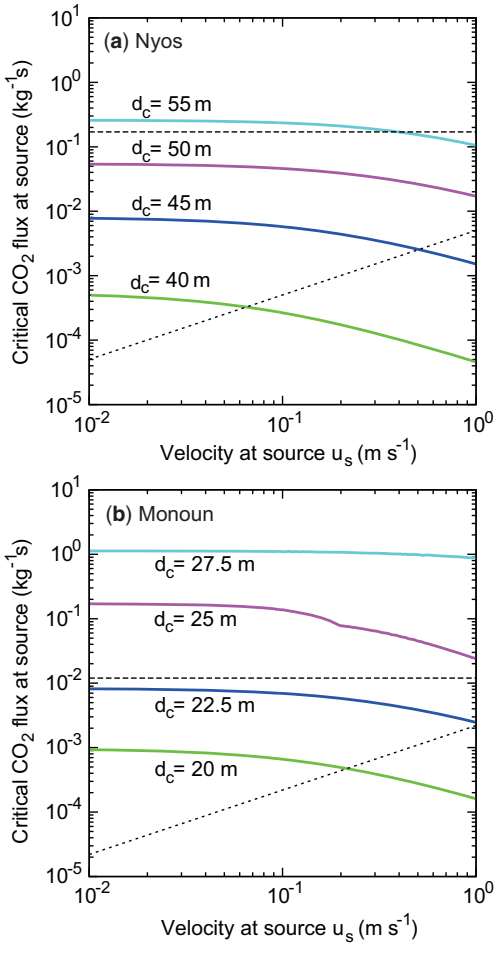

Fig. 3. Numerical results of the modeling of plume rise from mid-depths (solid circles in Fig. 2) of the lakes. A critical CO_2 flux at the source (mid-depth of the lake) for the bubble plume to reach the lake surface with an ascent velocity higher than 0.01 m s^{-1} throughout the lake, as a function of initial plume velocity at the source (u_s) is shown. Results are presented for lakes (**a**) Nyos and (**b**) Monoun with varying d_c. Dashed lines correspond to observed supply rates of CO_2 (Kusakabe *et al.* 2008), and dotted lines show the relationship between the CO_2 flux at the source and the initial velocity for an initial plume radius of 1 cm.

Nyos and 0.012 kg s^{-1} for Lake Monoun; Kusakabe *et al.* 2008) for a wide range of initial velocities. Although the critical flux becomes greater than the supply rate with increasing d_c, it is nevertheless much lower than the critical flux at the lake bottom for the plume to reach the lake surface under CO_2 profile in the lake based on the regular monitoring data (Table 1). Furthermore, when the plume reaches the surface, the surface flux of CO_2 becomes greater than the flux at the source (Fig. 4) because of the entrainment of CO_2 in the ambient water during ascent of the plume, as was also reported by Woods & Phillips (1999). These results indicate that the ascent of a bubble plume caused by the upward growth of the CO_2-undersaturated layer is a possible mechanism for inducing a limnic eruption.

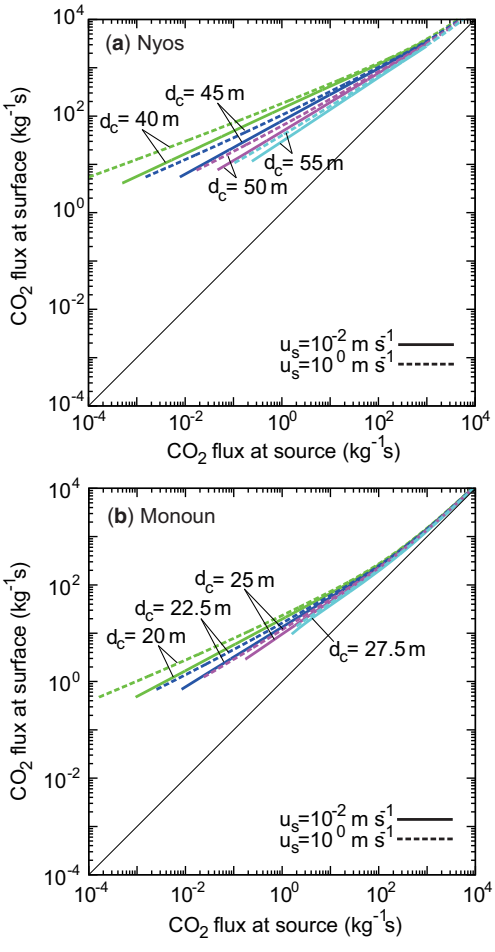

Fig. 4. Relationships between CO_2 flux at the lake surface and that at the source (mid-depths of the lakes) obtained from the model of plume rise from mid-depths of the lakes. Results are shown for lakes (**a**) Nyos and (**b**) Monoun with varying u_s and d_c. A solid line corresponds to the case in which the source flux is equal to the surface flux.

Dynamics of degassing pipe flow

Next we investigate the effects of the observed change in the CO_2 concentration at the bottom layer of the lake on the dynamics of degassing pipe flow by developing a numerical model. As the water containing CO_2 is withdrawn through a pipe from the bottom layer, bubble nucleation and expansion occur in the rising water in the pipe because of decompression, leading to a self-sustaining and steady two-phase (CO_2 bubble and water) flow. The flow that is ejected from the pipe mouth forms a fountain at the lake surface, as observed at both lakes. We also investigated numerically how features of the fountain, such as height, depend on the dynamics of pipe flow.

We adopted a model of one-dimensional steady flow through a cylindrical pipe with a constant radius, which is based on a conduit flow model for explosive volcanic eruptions (e.g. Wilson *et al.* 1980; Koyaguchi 2005). By treating the two-phase flow in the pipe as an apparent single-phase flow, under the assumption of no relative motion between the bubbles and water, the basic equations for the above model are expressed as follows:

$$\frac{\mathrm{d}(\rho u)}{\mathrm{d}z} = 0 \tag{1}$$

$$\rho u \frac{\mathrm{d}u}{\mathrm{d}z} = -\frac{\mathrm{d}p}{\mathrm{d}z} - \rho g - \frac{f\rho u^2}{2D} \tag{2}$$

$$\frac{1}{\rho} = \frac{1-n}{\rho_\mathrm{w}} + \frac{nRT}{p} \tag{3}$$

$$n = \frac{n_0 - c(p)}{1 - c(p)} \tag{4}$$

$$\frac{1}{\sqrt{f}} = -1.8\log_{10}\left[\left(\frac{\varepsilon}{3.7D}\right)^{1.11} + \frac{6.9}{\mathrm{Re}}\right] \tag{5}$$

where ρ is the density of the bubble–water mixture, u is the velocity, z is the vertical coordinate measured positive upwards, p is the pressure, g is acceleration due to gravity, f is the friction coefficient, D is the diameter of the pipe (in m), n is the mass fraction of CO_2 gas, ρ_w is the density of water (1000 kg m^{-3}), R is the gas constant (189 J kg^{-1} K^{-1} for CO_2 gas), T is the temperature (set to be 298 K in this study), n_0 is the initial CO_2 concentration (mass fraction) at the source, $c(p)$ is the mass fraction of CO_2 dissolved in water (i.e. solubility) obtained from Duan & Sun (2003), and ε is the roughness of the pipe (1.5×10^{-6} m for plastic piping; Moody 1944). Here, Re in equation (5) is the Reynolds number, expressed as $\rho u D/\eta$ where η is the viscosity of water, set to be 10^{-3} Pa s.

Equations (1) and (2) describe the mass and momentum conservation respectively, equation (3) is the equation of state for the bubble–water mixture, and equation (4) represents the mass fraction of CO_2 gas when equilibrium gas exsolution is assumed. Equation (5) is the form of the friction coefficient for a pipe given by Haaland (1983), which is valid for values of Re ranging from 5×10^3 to 1×10^8. Because the value of Re in the pipe flow at lakes Nyos and Monoun is roughly estimated to be in this range, the formulation of

equation (5) is appropriate for the modelling. The above equations are solved as a two-point boundary value problem for a given pipe with length L. The boundary condition at the bottom end of the pipe is that the pressure is equal to the hydrostatic pressure at the pipe intake depth. The boundary condition at the exit of the pipe is that the pressure is equal to the atmospheric pressure (about 9×10^4Pa for both lakes) for subsonic flow, or the flow velocity is equal to the sound velocity of the mixture. This sound velocity (a) is expressed under the assumption that the sound velocity under isentropic condition is approximated by that under isothermal condition as (e.g. Kieffer 1977):

$$a \equiv \sqrt{\frac{\mathrm{d}p}{\mathrm{d}\rho}} \sim \sqrt{\frac{p}{\phi\rho}} = \frac{p}{\rho\sqrt{nRT}}, \qquad (6)$$

where ϕ is the volume fraction of gas expressed by $\rho nRT/p$. Using equations (1) and (6), equation (2) is rewritten as (e.g. Koyaguchi 2005):

$$\frac{\mathrm{d}p}{\mathrm{d}z} = -\frac{\rho g + (f\rho u^2/2D)}{1 - (u^2/a^2)}. \qquad (7)$$

This equation indicates that the pressure gradient $\mathrm{d}p/\mathrm{d}z$ diverges to infinity at the exit when $u = a$, which corresponds to a 'choking condition'.

Currently, in each lake three degassing pipes are installed, for which the lengths (L) and/or the diameters (D) are different (Halbwachs *et al.* 2004; Kusakabe *et al.* 2008). At Lake Nyos, one pipe with $L = 203$ m and $D = 14.5$ cm was installed in 2001, and two pipes with $L = 203$ m and $D = 25.7$ cm were added in 2011. At Lake Monoun, one pipe with $L = 73$ m and $D = 10$ cm was installed in 2003. Two pipes with $L = 93$ m and $D = 10$ cm were added in 2006, at which time the length of the existing pipe was changed to 93 m. We use these values of L and D in the calculations below.

Figure 5 shows typical numerical results using our model for the pipe flow. As the water pressure decreases during ascent through the pipe (Fig. 5a), exsolution of CO_2 gas starts at the mid-depth of the pipe (118 m) where the water reaches a state of CO_2-saturation (Fig. 5b). Further ascent leads to an increase in the volume fraction of the gas (Fig. 6b) and a large increase in the velocity of outflow (Fig. 5c). The profiles of the gas volume fraction and the velocity depend strongly on the initial CO_2 concentration at the pipe intake depth n_0 (Fig. 5b, c).

Figure 6 shows how the features of the pipe flow depend on the CO_2 concentration at the pipe inlet. The velocity and the gas volume fraction at the exit increase dramatically with n_0 (Fig. 6a, b), because the increase in n_0 promotes gas expansion and acceleration of the pipe flow (Fig. 5b, c). The increase in the velocity also leads to an increase in the mass fluxes of water and CO_2 (Fig. 6d). The curves in Figure 6a and b show a bend in the region where n_0 is about 0.01. This bend is caused by the change in the boundary condition at the exit. In the case where n_0 is small (<0.01), the boundary condition is that the pressure is equal to atmospheric (Fig. 6c) and, in this case, the flow reaches the surface as a subsonic flow. On the other hand, when n_0 is large (>0.01), the boundary condition is that the exit velocity is equal to the sonic velocity, whereas the pressure is greater than atmospheric (Fig. 6c). Although the mass flux of the water or CO_2 strongly depends on D because the flux increases with pipe

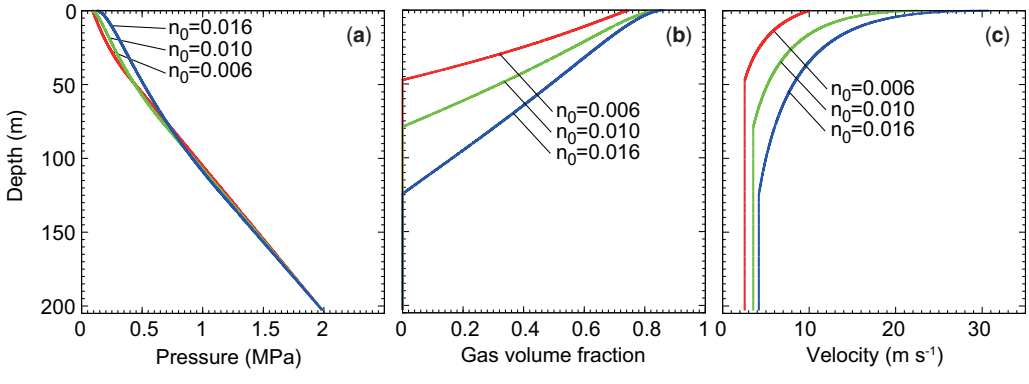

Fig. 5. Typical numerical results of the distributions of (**a**) pressure, (**b**) gas volume fraction, and (**c**) velocity inside the degassing pipe obtained from the pipe flow model (Equations (1)–(5)). The length and diameter of the pipe are set at 203 m and 14.5 cm, respectively, by referencing the pipe in Lake Nyos. Results are obtained for varying CO_2 concentrations at the pipe inlet (n_0).

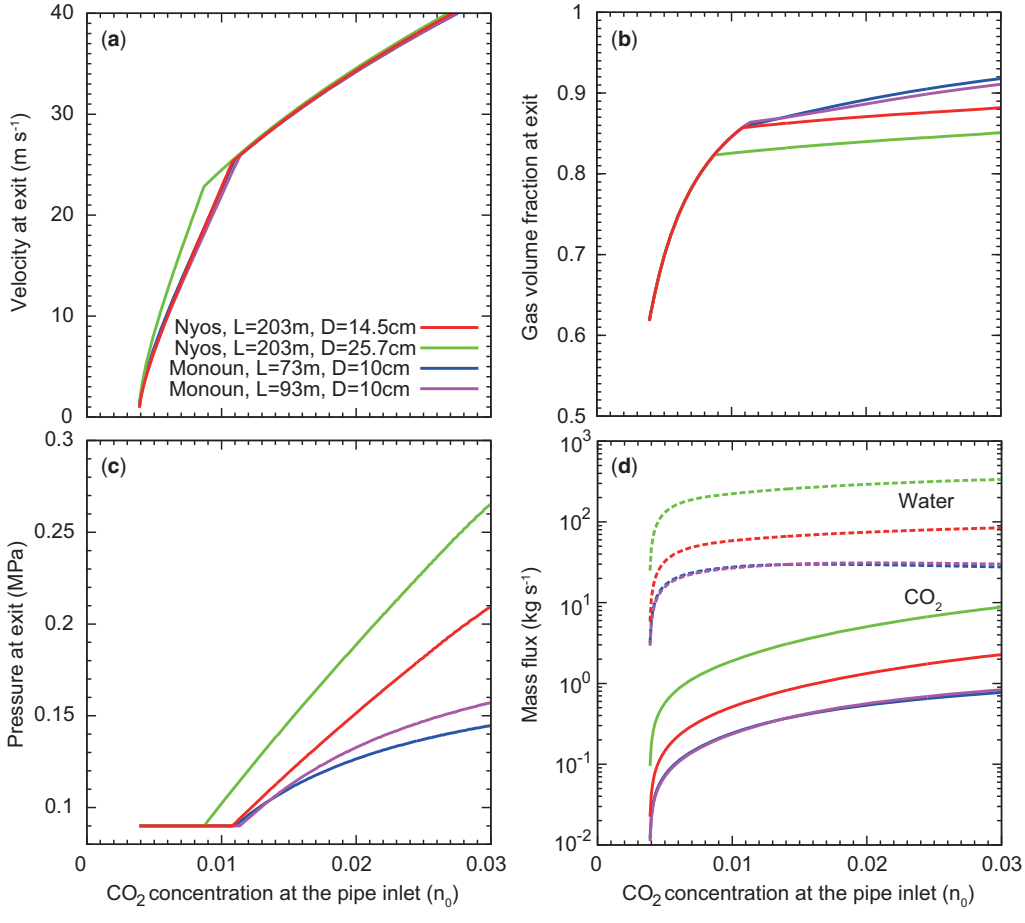

Fig. 6. Variations of (**a**) velocity, (**b**) gas volume fraction, (**c**) pressure at the exit of the degassing pipe, and (**d**) mass fluxes of CO_2 (solid curves) and water (dashed curves) in the pipe, as a function of n_0. The length (L) and the diameter (D) of the pipe are varied depending on the pipes installed in lakes Nyos and Monoun.

diameter (Fig. 6d), the velocity and the gas volume fraction at the exit are affected only slightly by variations in L and D (Fig. 6a, b).

Using the exit velocity obtained in our calculations (Fig. 6a), we can estimate the height of the fountain (H; Fig. 7) using the relationship $H = u_e^2/(2\,g)$, where u_e is the exit velocity. As shown in the variation of the exit velocity (Fig. 6a), the fountain height also increases dramatically with n_0, and it weakly depends on L and D (Fig. 7). Because the fountain height is directly observable at the surface, we can compare the observed heights with the numerical results in Figure 7. The value of n_0 at the time the fountain is observed is estimated from the CO_2 monitoring data at the pipe intake depth (203 m for Lake Nyos and 73 or 93 m for Lake Monoun) (Fig. 8). Except for the observations made during January 2009 at Lake Nyos and during December 2007 at Lake Monoun, our results agree well with the observed heights for a wide range of n_0 (Fig. 7), indicating that our model is successful in capturing the dynamics of the degassing pipe flow in lakes Nyos and Monoun. It should be noted that the good agreement in Figure 7 was achieved without adjusting any of the parameters in the pipe flow model. The origin of the differences between our results and the observations in Figure 7 will be discussed below.

Discussion

Our numerical results using the bubble plume model show that a bubble plume generated from the mid-depth of the lake can reach the lake surface with a high flux of CO_2 under realistic conditions. We

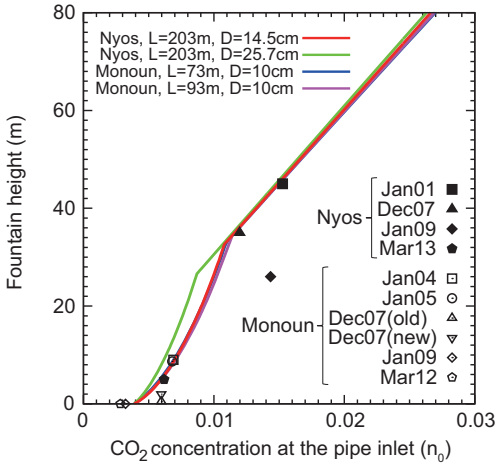

Fig. 7. Variation of the height of the fountain generated from the degassing pipe as a function of n_0. The results for the same simulations as in Figure 6. The observed fountain heights v. the CO_2 concentrations at the pipe inlet at the time of fountain observation are also plotted.

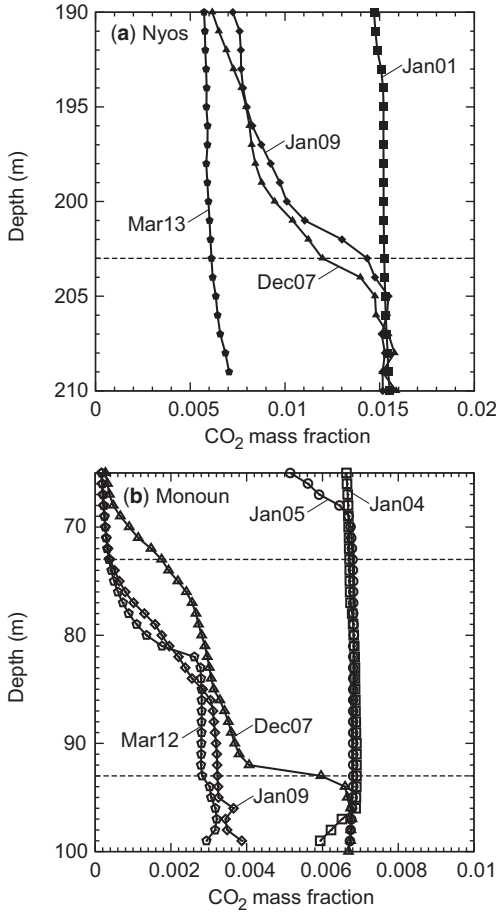

Fig. 8. Enlarged view of CO_2 profiles at lakes (**a**) Nyos and (**b**) Monoun around the pipe inlet depth (203 m for Lake Nyos, and 73 or 93 m for Lake Monoun; dashed lines). The data used for the observations plotted in Figure 7 are shown here.

consider that this is a likely mechanism for a limnic eruption. However, in order to prime the plume from mid-depths, a certain amount of upwards flux or velocity is necessary, and such an increase in the flux or the velocity may be caused by a localized upwards movement of the CO_2-saturated water from the top of the growing layer. Three-dimensional measurements at Lake Nyos have shown a clear stratification with horizontally homogeneous layers (Kusakabe *et al.* 2008), and the horizontal homogeneity presents a difficulty for local perturbations to occur. In addition, the velocity of the upwards growth of the bottom layer, which can be estimated from the evolution of the CO_2 profiles before controlled degassing, is too low to generate the plume (Fig. 1a, d).

There are some possible mechanisms for generating a local perturbation at the top of the growing layer. One is a perturbation of the layer boundary caused by double-diffusive convection. Schmid *et al.* (2004) investigated the susceptibility of lake water to double-diffusive convection on the basis of the CO_2 and temperature profiles at Lake Nyos, and they showed that double-diffusive convection was most likely to take place in the region near the chemoclines. In our scenario, the top of the growing layer exists at the lower chemocline (Fig. 1, d), and destabilization of the layer boundary by double-diffusive convection may be a trigger for localized upwards movement of CO_2-saturated water and subsequent plume generation. To assess the potential for this destabilization, it is necessary to monitor both the CO_2 and the temperature profiles inside the lakes with high resolution (Kusakabe *et al.* 2008). Other mechanism is a perturbation caused by internal waves due to either a storm or a sediment mass movement (e.g. Kling *et al.* 1987). The limnic eruptions in the 1980s at lakes Nyos and Monoun occurred during the rainy season in August, and earthquake-triggered landslide is reported for Monoun (Sigurdsson *et al.* 1987). These observations imply that the internal wave is also a possible trigger mechanism. Local perturbation may also be caused by a seiche, which is induced by external forcings such as strong wind.

We have shown in Figure 3 that the critical flux for the CO_2 plume to reach the surface dramatically

increases with increasing d_c. Because whether the plume ascends or not is mainly determined in the region near the source (i.e. the mid-depth of the lake), the results in Figure 3 imply that the CO_2 profile near the source largely affects the critical condition for limnic eruptions. In our analyses, we assumed a simplified linear CO_2 profile near the source. The actual profile, however, may be more complex, as deduced from the regular monitoring data (Fig. 1). If the profile keeps its shape during upwards growth of bottom layer, the CO_2 concentration near the source is further away from saturation than in the assumed linear profile. The critical CO_2 flux in this case would be higher. If a plume occurs that is not sufficient to reach the surface, it will nevertheless increase CO_2 concentrations (by bubble dissolution) above the chemocline and thus facilitate the rise of a future plume. Although it is unclear how the profile evolves during the growth of the layer, this evolution process is another key factor controlling the conditions for limnic eruptions.

On the basis of the numerical model for degassing pipe flow, we obtained a quantitative relationship between CO_2 concentration at the pipe inlet and fountain height (Fig. 7). Because the fountain height is sensitive to the CO_2 concentration of intake water, the relationship in Figure 7 is useful for estimating the CO_2 concentration at the bottom of the lake from the fountain height, which is easily observable. Although our results agree with most of the observational data, the observations in January 2009 at Lake Nyos and in December 2007 at Lake Monoun deviate from the model predictions (Fig. 7). One likely reason for this deviation is an error in estimating the CO_2 concentration at the pipe inlet n_0 from the monitoring data, because the pipe intake depths in January 2009 at Lake Nyos (203 m) and in December 2007 at Lake Monoun (93 m) were close to the chemocline where CO_2 concentrations change dramatically (Fig. 8). This fact might generate errors in estimating n_0. In order to reproduce the observed fountain heights in January 2009 at Lake Nyos and in December 2007 at Lake Monoun, n_0 should be about 0.01 and 0.005, respectively (Fig. 7). These values of the CO_2 concentrations were observed at a depth of about 200 m depth for Lake Nyos (January 2009) and 92.5 m for Lake Monoun (December 2007) (Fig. 8). Because the difference between the depth for Lake Nyos and the actual pipe inlet depth is as large as 3 m, a local perturbation of the chemocline near the pipe inlet may be another reason for the deviation in Figure 7.

The numerical results for pipe flow allow us to assess the quantitative contribution of the degassing pipe to the decrease in CO_2 in the lake. On the basis of the evolution of the total exsolved CO_2 in the lake, calculated from the regular monitoring data, Kusakabe *et al.* (2008) estimated the rate of CO_2 accumulation at Lake Nyos during 1986–2001 and at Lake Monoun during 1993–2003 before controlled degassing was introduced, and they also estimated the rate of decrease in CO_2 (i.e. net change of CO_2 in the lake volume) during the controlled degassing in 2001–06 at Lake Nyos and in 2003–06 and 2006–07 at Lake Monoun (two new pipes were installed in 2006 at Monoun) (Table 2). We can calculate the CO_2 flux inside the pipe (referred to as the 'degassing rate'; Table 2) using the CO_2 flux–n_0 relationship in Figure 6d, where the value of n_0 was determined from the monitoring data at the pipe inlet (Fig. 8). Here the degassing rate in Mmol a^{-1} in Table 2 was calculated from that in units of kg s^{-1} in Figure 6d.

If the degassing pipe works perfectly, and if the gas accumulation rate during controlled degassing is the same as that before the controlled degassing, the rate of decrease in CO_2 would be equal to the sum of the accumulation and degassing rates (i.e. the accumulation rate + the degassing rate = the rate of decrease in CO_2). At Lake Nyos, this relationship is well satisfied, but at Lake Monoun the magnitude of the sum of the accumulation and degassing rates is larger than that of the rate of decrease in CO_2 (though they are of the same order of magnitude). At least three factors could have contributed to

Table 2. *Degassing rates of lakes Nyos and Monoun estimated from the calculation of CO_2 flux inside the pipe by numerical model (Fig. 6d), and CO_2 accumulation rates before controlled degassing and rates of decrease in CO_2 during controlled degassing estimated by Kusakabe et al. (2008)*

	Lake Nyos	Lake Monoun
Degassing rate	−676 (2001–06)	−98 (2003–06) −282 (2006–07)
Accumulation rate	120 ± 40 (1986–2001)	8.4 ± 3.6 (1993–2003)
Rate of decrease in CO_2	−590 ± 150 (2001–06)	−61.7 ± 8.9 (2003–06) −182.0 ± 13.0 (2006–07)

Units are Mmol a^{-1}.

this discrepancy. The first is that our model of pipe flow overestimates the degassing rate, as shown in the difference between the model predictions of fountain height and some observations (Fig. 7). The second factor is that the calculation of the degassing rate in Mmol a^{-1} from that in kg s^{-1} assumes permanent operation of the degassing pipes, while in reality, the degassing was occasionally interrupted for maintenance (e.g. Schmid *et al.* 2006), leading to a decrease in the effective degassing rate. The third factor is the possibility that the supply rate of CO_2 into the lake during controlled degassing was higher than that beforehand. To estimate the CO_2 supply rate during controlled degassing, it is important to know the total duration of operation.

In 2007 and 2008 at Lake Monoun the fountain heights at the three pipes were simultaneously measured, and interestingly, the heights were different from pipe to pipe. This difference was observed not only in December 2007 at the same time as the regular monitoring (Fig. 7), but also in the period from June 2007 to February 2008 when the fountain heights were measured monthly. The differences of the fountain heights between the pipes were seemingly random, not systematic. The three pipes at Lake Monoun have the same lengths and diameters, and the regular monitoring data for CO_2 in 2007 show that the depth of the pipe inlet was close to the chemocline (Fig. 8b). We consider, therefore, that one reason for the difference in fountain height is a spatial heterogeneity of CO_2 concentration at the pipe inlet depth possibly caused by a small perturbation of the chemocline. This indicates that monitoring of fountain height is useful for detecting local changes in the CO_2 concentration at the lake bottom. Differences in fountain height have also been observed among the pipes at Lake Nyos in 2013, and consistently the heights at the new pipes were slightly higher than at the old pipe. We consider that this difference is caused by the differences in pipe diameter (25.7 cm for the new pipes and 14.5 cm for the old pipe), and our model predicts that the fountain height increases slightly with pipe diameter (Fig. 7) because of the lower relative importance of wall friction compared to buoyancy in a larger pipe.

Finally, it should be noted that when the thickness of the bottom CO_2-rich layer of the lake increases because of the supply of CO_2-undersaturated fluid, as shown in our scenario, the fountain height generated by the degassing pipe should remain unchanged because the CO_2 concentration at the pipe inlet is constant. Therefore, although we can obtain basic information about CO_2 concentrations at the lake bottom from fountain heights using the model predictions in Figure 7, we consider that regular monitoring of the CO_2 profile in the lake (as in Fig. 1) is essential and fundamental for detecting a possible increase in the potential for limnic eruptions.

Conclusions

We have investigated the potential for limnic eruptions at lakes Nyos and Monoun on the basis of numerical modeling and regular monitoring of the CO_2 in the lakes. The evolution of the CO_2 profiles indicated the following likely scenario for a limnic eruption: a continuous supply of CO_2-undersaturated fluid from the lake bottom induces an upwards growth of the CO_2-rich bottom layer to middle depths where CO_2 concentration eventually reaches saturation and bubble formation follows. By using the numerical model for the ascent of a plume of CO_2 bubbles, we found that under realistic conditions the bubble formation in the above scenario leads to a bubble plume reaching the lake surface with a high CO_2 flux, which corresponds to a limnic eruption. We also developed a numerical model for degassing pipe flow so that we could investigate the effects of changes in CO_2 concentration at the lake bottom on the dynamics of the pipe flow and the degree of degassing. This model allowed us to obtain the relationship between CO_2 concentration at the lake bottom and fountain height observed on the surface of the lake. To undertake a more quantitative investigation of the mechanism of limnic eruptions, as proposed in this study, it is necessary to model the process by which the CO_2-rich bottom layer grows upwards, caused by a continuous supply of CO_2-undersaturated fluid from the bottom. Further analysis of this process is important for better understanding of the dynamics of limnic eruptions.

We thank an anonymous reviewer for insightful comments and suggestions that greatly improved the manuscript. This research was supported by JST/JICA sponsored SATREPS project 'Magmatic fluid supply into Lakes Nyos and Monoun, and mitigation of natural disasters through capacity building in Cameroon' (2011–16, headed by T. Ohba).

References

Duan, Z. & Sun, R. 2003. An improved model calculating CO_2 solubility in pure water and aqueous NaCl solutions from 273 to 533 K and from 0 to 2000 bar. *Chemical Geology*, **193**, 257–271.

Evans, W.C., White, L.D., Tuttle, M.L., Kling, G.W., Tanyileke, G. & Michel, R.L. 1994. Six years of change at Lake Nyos, Cameroon, yield clues to the past and cautions for the future. *Geochemical Journal*, **28**, 139–162.

Giggenbach, W.F. 1990. Water and gas chemistry of Lake Nyos and its bearing on the eruptive process.

Journal of Volcanology and Geothermal Research, **42**, 337–362.

HAALAND, S.E. 1983. Simple and explicit formulas for the friction factor in turbulent pipe flow. *Journal of Fluids Engineering*, **105**, 89–90.

HALBWACHS, M., SABROUX, J.C. *ET AL.* 2004. Degassing the 'Killer Lakes' Nyos and Monoun, Cameroon. *EOS*, **85**, 281–288.

KANTHA, L.H. & FREETH, S.J. 1996. A numerical simulation of the evolution of temperature and CO_2 stratification in Lake Nyos since the 1986 disaster. *Journal of Geophysical Research*, **101**, 8187–8203.

KIEFFER, S. 1977. Sound speed in liquid–gas mixtures: water–air and water–stream. *Journal of Geophysical Research*, **82**, 2895–2904.

KLING, G.W., CLARK, M.A. *ET AL.* 1987. The 1986 Lake Nyos gas disaster in Cameroon, West Africa. *Science*, **236**, 169–175.

KLING, G.W., TUTTLE, M.L. & EVANS, W.C. 1989. The evolution of thermal structure and water chemistry in Lake Nyos. *Journal of Volcanology and Geothermal Research*, **39**, 151–165.

KOYAGUCHI, T. 2005. An analytical study for 1-dimensional steady flow in volcanic conduits. *Journal of Volcanology and Geothermal Research*, **143**, 29–52.

KUSAKABE, M. 2015. Evolution of CO_2 content in Lakes Nyos and Monoun, and sub-lacustrine CO_2-recharge system at Lake Nyos as envisaged from $CO_2/^3He$ ratios and noble gas signatures. *Volcanic Lakes*, 427–450.

KUSAKABE, M., OHSUMI, T. & ARAMAKI, S. 1989. The Lake Nyos gas disaster: chemical and isotopic evidence in waters and dissolved gases from three Cameroonian crater lakes, Nyos, Monoun and Wum. *Journal of Volcanology and Geothermal Research*, **39**, 167–185.

KUSAKABE, M., TANYILEKE, G., MCCORD, S.A. & SCLADOW, S.G. 2000. Recent pH and CO2 profiles at Lakes Nyos and Monoun, Cameroon: implications for the degassing strategy and its numerical simulation. *Journal of Volcanology and Geothermal Research*, **97**, 241–260.

KUSAKABE, M., OHBA, T. *ET AL.* 2008. Evolution of CO_2 in Lakes Monoun and Nyos, Cameroon, before and during controlled degassing. *Geochemical Journal*, **42**, 93–118.

MOODY, L.F. 1944. Friction factors for pipe flow. *Transactions of the American Society of Mechanical Engineers*, **66**, 671–684.

MOTT, R.W. & WOODS, A.W. 2010. A model of overturn of CO_2 laden lakes triggered by bottom mixing. *Journal of Volcanology and Geothermal Research*, **192**, 151–158.

RICE, A. 2000. Rollover in volcanic crater lakes: a possible cause for Lake Nyos type disasters. *Journal of Volcanology and Geothermal Research*, **97**, 233–239.

SCHMID, M., LORKE, A., DINKEL, C., TANYILEKE, G. & WÜEST, A. 2004. Double-diffusive convection in Lake Nyos, Cameroon. *Deep Sea Research Part I*, **51**, 1097–1111.

SCHMID, M., HALBWACHS, M. & WUEST, A. 2006. Simulation of CO_2 concentrations, temperature, and stratification in Lake Nyos for different degassing scenarios. *Geochemistry, Geophysics, Geosystems*, **7**, Q06019. https://doi.org/10.1029/2005GC001164

SIGURDSSON, H., DEVINE, J.D., TCHOUA, F.M., PRESSOR, T.S., PRINGLE, M.K.W. & EVANS, W.C. 1987. Origin of the lethal gas burst from Lake Monoun, Cameroun. *Journal of Volcanology and Geothermal Research*, **31**, 1–16.

SIGVALDASON, G.E. 1989. International conference on Lake Nyos disaster, Yaounde, Cameroon 15–20 March 1987: conclusions and recommendations. *Journal of Volcanology and Geothermal Research*, **39**, 97–107.

YOSHIDA, Y., ISSA KUSAKABE, M., SATAKE, H. & OHBA, T. 2010. An efficient method for measuring CO_2 concentration in gassy lakes: application to Lakes Nyos and Monoun, Cameroon. *Geochemical Journal*, **44**, 441–448.

WILSON, L., SPARKS, R.S.J. & WALKER, G.P.L. 1980. Explosive volcanic eruptions: IV. The control of magma properties and conduit geometry on eruption column behaviour. *Geophysical Journal of the Royal Astronomical Society*, **63**, 117–148.

WOODS, A.W. & PHILLIPS, J.C. 1999. Turbulent bubble plumes and CO_2 driven lake eruptions. *Journal of Volcanology and Geothermal Research*, **92**, 259–270.

ZHANG, Y. 1996. Dynamics of CO_2-driven lake eruptions. *Nature*, **379**, 57–59.